

1  
2  
3  
4  
5  
6  
7  
8  
9  
10  
11  
12  
13  
14  
15  
16  
17  
18  
19  
20  
21  
22

**Diffusion Tensor Tractography  
of Traumatic Diffuse Axonal Injury**

Jun Yi Wang,<sup>1</sup> Khamid Bakhadirov,<sup>1</sup> Michael D. Devous, Sr.,<sup>2</sup> Hervé Abdi,<sup>1</sup> Roddy McColl,<sup>2</sup>  
Carol Moore,<sup>2</sup> Carlos D. Marquez de la Plata,<sup>2</sup> Kan Ding,<sup>2</sup> Anthony Whittemore,<sup>2</sup> Evelyn  
Babcock,<sup>2</sup> Tiffany Rickbeil,<sup>2</sup> Julia Dobervich,<sup>2</sup> David Kroll,<sup>2</sup> Bao Dao,<sup>2</sup> Nisha Mohindra,<sup>2</sup>  
Ramon Diaz-Arrastia<sup>2</sup>

*1. The University of Texas at Dallas, Richardson, TX, USA*

*2. University of Texas Southwestern Medical Center, Dallas, TX, USA*

Correspondence: Dr. Ramon Diaz-Arrastia

Address: Department of Neurology, UT Southwestern Medical Center at Dallas; 5323 Harry

Hines Blvd, Dallas, Texas 75390-9063

Tel: 214-648-6721, Fax: 214-648-6320

Email: [ramon.diaz-arrastia@utsouthwestern.edu](mailto:ramon.diaz-arrastia@utsouthwestern.edu)

Date of revision: Oct. 1, 2007

Word Count: text with tables, 4657; text (not including tables), 3662

23  
24  
25  
26  
27  
28  
29  
30  
31  
32  
33  
34  
35  
36  
37  
38  
39  
40  
41  
42  
43  
44

### Abstract

**Objectives:** Diffuse axonal injury is a common consequence of traumatic brain injury that frequently involves the parasagittal white matter, corpus callosum, and brain stem. This study examined the potential of diffusion tensor tractography in detecting diffuse axonal injury at the acute stage and predicting long-term functional outcome. **Design:** Tract-derived fiber parameters were analyzed to distinguish patients from controls and to determine their relationship to outcome. **Setting:** Inpatient traumatic brain injury unit. **Patients or other participants:** 12 patients were scanned approximately 7 days after injury; 12 age- and gender-matched controls were also scanned. **Main outcome measure:** Six fiber parameters of the corpus callosum, fornix, and peduncular projections were obtained. Glasgow outcome scale-extended was assessed approximately 9 months post-injury in 11/12 patients. **Results:** At least one fiber parameter of each region showed diffuse axonal injury-associated alterations. At least one fiber parameter of the anterior body and splenium of the corpus callosum correlated significantly with the Glasgow outcome scale-extended scores. The predicted outcome scores correlated significantly with actual scores in a mixed effects model. **Conclusions:** Diffusion Tensor Tractography-based quantitative analysis of acute MRI scans has the potential to serve as a valuable biomarker of diffuse axonal injury and predict long-term outcome.

45  
46  
47  
48  
49  
50  
51  
52  
53  
54  
55  
56  
57  
58  
59  
60  
61  
62  
63  
64  
65  
66  
67

## Introduction

Traumatic brain injury (TBI) is a major cause of mortality and disability. In the United States alone, more than 1.4 million cases are reported annually along with 235,000 hospitalizations and 50,000 deaths.<sup>1</sup> Diffuse axonal injury (DAI) is the predominant mechanism of the injury in 40-50% of TBI cases that require hospitalization<sup>2</sup> and is likely a factor in most cases resulting from high-speed motor vehicle collisions. DAI is a consequence of sustained acceleration/deceleration forces that can shear axons and produce microscopic changes in the brain. In humans, the primary cytoskeleton disorganization can be observed through histological examinations between 4-6 hours post-injury. Secondary axotomy normally starts from 12 hours post-injury,<sup>3</sup> peaks between 1-3 days, and may last for years.<sup>4,5</sup> DAI is a multifocal injury primarily affecting the parasagittal WM, corpus callosum (CC), and brain stem.<sup>2,3,6</sup>

Fluid Attenuation and Inversion Recovery (FLAIR) imaging can be useful in identifying DAI. We reported that FLAIR lesion volume acquired within two weeks of the injury correlated moderately with long-term functional outcome, Glasgow Outcome Scale-Extended (GOSE).<sup>7</sup> Susceptibility-weighted imaging (SWI) is more sensitive than T2-weighted gradient-echo images in detecting hemorrhagic DAI<sup>8-10</sup> and the quantity and volume of SWI hemorrhages examined at the acute stage correlated well with dichotomized long-term outcome in pediatric TBI patients.<sup>11</sup> A novel MRI technique, diffusion tensor imaging (DTI), permits the examination of WM integrity *in vivo* through observing the amount of water diffusion within biological tissues.<sup>10,12</sup> A direct comparison between DTI-detected WM integrity changes and histological findings in an animal model of axonal injury<sup>13</sup> suggests that DTI may become a valuable imaging tool for detecting DAI.

68

69 Two diffusion parameters have been used<sup>14</sup> for characterizing WM integrity, namely fractional  
70 anisotropy (FA), a ratio from 0-1 that represents the degree of alignment of the underlying fibers  
71 in a voxel, and mean diffusivity (MD) that represents the presence of overall restrictions to water  
72 diffusion. Two studies<sup>15, 16</sup> have applied DTI-based regions of interest (ROI) analyses in  
73 assessing DAI during the acute stage and found loss of structural integrity in CC, internal and  
74 external capsules, and centrum semiovale. Diffusion tensor tractography (DTT)-based  
75 quantification may have advantages over ROI-based DTI analysis.<sup>17</sup> In DTT, the whole length  
76 of WM structures of interest can be three-dimensionally (3D) reconstructed through fiber  
77 propagation algorithms and associated fiber measurements can be obtained. DTT-based  
78 quantification has been applied in group analyses in chronic adult<sup>18</sup> and pediatric TBI patients<sup>19</sup>  
79 and revealed loss of structural integrity in CC. However, an association between DTI  
80 measurements and long-term outcome was only found in chronic TBI patients using either  
81 ROI<sup>20</sup>- or DTT<sup>19</sup>-based approach.

82

83 The goal of the current study was to evaluate DTT as a tool for detecting DAI at an early  
84 pathological stage when the injury process was still ongoing and potentially reversible by  
85 therapeutic intervention and identify measures associated with long-term functional outcome.  
86 We hypothesized that fiber parameters of three commonly affected WM tracts (CC, fornix, and  
87 peduncular projections (PP)) would correlate better with outcome than standard measures of  
88 injury severity and FLAIR-based measurement of white matter hyperintensity volume (WMH).

89

90

**Methods**91 *Subjects*

92 Twelve TBI patients were recruited from Parkland Memorial Hospital, Dallas, Texas. Inclusion  
93 criteria required that patients: 1) sustained severe closed-head traumatic brain injury; 2) injury  
94 mechanism was consistent with DAI; 3) had ability to provide consent or consent was provided  
95 by legal guardian; 4) had at least an 8<sup>th</sup> grade education; and 5) were at least 16 years old.

96 Patients with preexisting neurologic disorders or previous brain injury were excluded from the  
97 study. One patient was lost to follow up. Eleven age- and gender-matched normal controls with  
98 good general health and no known neurocognitive disorders were also recruited.

99

100 *Functional Outcome Measure*

101 Functional outcomes were determined at least 6 months post-injury using the GOSE.<sup>21</sup> The  
102 GOSE is a commonly used questionnaire that assesses functional abilities in multiple domains  
103 following a head injury and has shown to be a reliable outcome measure.<sup>22</sup> All outcome  
104 interviews and scoring of the GOSE were conducted by one of three study coordinators, who  
105 were blind to the imaging results. Each rater had at least a bachelor's level education and at least  
106 1-month experience in working with TBI patients. Each was trained by a neurologist (RD-A) by  
107 observing in-person administration of at least five subjects, as well as by over-the-telephone  
108 administration for five subjects. A structured questionnaire was used during the follow-up  
109 interviews.<sup>21</sup> Each subject was interviewed only once. Inter-rater reliability for scoring the  
110 GOSE was assessed by auditing 20% of the scoring sheets every three months. Reproducibility  
111 has been > 99%. Questionnaires were answered by patients, although in case of death or other

112 severe disability, completion by a caregiver was accepted. Total GOSE scores range from one to  
113 eight, with higher scores indicating better outcome.

114

#### 115 *Image Acquisition and Processing*

116 DTI, T1-weighted, and FLAIR images were acquired on a GE Signa Excite 3T MRI scanner.

117 The DTI sequences were obtained using a single-shot spin-echo, echo-planar imaging sequence

118 with FOV 240 mm, slice thickness/gap 3/0 mm, ~45 slices, TR/TE 12,000/75.5 ms, flip angle 90,

119 NEX 2, matrix 128×128. The diffusion sensitizing gradients were applied at a *b*-value of 1,000

120 s/mm<sup>2</sup>/axis with 19 noncollinear directions and 3 *b*<sub>0</sub> images. The acquisition time was 9

121 minutes. Voxel size was 2×2×3 mm<sup>3</sup> interpolated (by default at the scanner) to 1×1×3 mm<sup>3</sup>. The

122 T1-weighted structural images were acquired using fast spoiled GRASS sequence with FOV 240

123 mm, slice thickness/gap 1.3/0 mm, ~130 slices, TE 2.4 ms, flip angle 25, NEX 2, matrix 256×92,

124 acquisition time 6 minutes. The FLAIR images were acquired at the axial plane using tailored

125 RF and fast spin echo sequence with FOV 200-210 mm, slice thickness/gap 3.0/0.5mm, ~ 28

126 slices, TR/TE/TI 9500/136.6/2500 ms, flip angle 90, NEX 1, matrix 320×224, acquisition time 4

127 minutes.

128

129 Preprocessing steps for the DTI images included realignment using DTI Studio (Johns Hopkins

130 Medical Institute, <http://lbam.med.jhmi.edu/>) and brain extraction and eddy-current correction

131 using FSL (<http://www.fmrib.ox.ac.uk/fsl/>). Intracranial volumes for normalizing fiber

132 parameters were calculated based on T1-weighted structural images using FSL. Diffusion map

133 generation, fiber tractography and quantification were performed in DTI Studio using a fiber

134 tracking threshold of FA 0.25 and angle 60°.

135

136 *Image Analyses*

137 Three WM structures susceptible to TBI were included in the analysis.<sup>15, 23, 24</sup> Fiber tracking  
138 adopted a multiple ROIs approach<sup>17, 25</sup> to increase accuracy and inter-rater reliability.

139 Anatomical landmarks for slice selections were defined rigorously to reduce subjectivity in fiber  
140 tracking. Because CC and PP are large fiber bundles connecting multiple brain regions, they  
141 were parcellated into sub-tracts for detecting DAI that might affect only a part of the tracts. CC  
142 was parcellated into four equal areas, CC1-4, corresponding to the genu, anterior and posterior  
143 body, and splenium of the CC. The parcellation of PP to ventral frontal (PVF), dorsal frontal  
144 (PDF), parietal (PPar) and occipital cortices (POcc) followed general guidelines of the CC  
145 parcellation.<sup>26</sup> The fornix body and left and right crura were tracked separately.<sup>27</sup> Figure 1  
146 shows representative fornix body ROIs of a control and a patient.

147

148 Each WM structure was tracked independently by two raters from a pool of five raters. Fiber  
149 parameters including mean FA, tensor trace (total diffusivity or  $3 \times$  mean diffusivity), fiber  
150 count, mean length, fiber volume, and fiber density index (FDI, fiber count/voxel) were  
151 recorded. Inter-rater reliabilities were measured with Pearson correlation coefficients and were  
152 above 96% for all fiber parameters except for those of fornix crus, which were above 87%. Fiber  
153 count and fiber volume were normalized using intracranial volume.

154

155 FLAIR image analysis followed previously published methods.<sup>7</sup> WMH volumes were estimated  
156 using in-house software and normalized with whole brain volume to create DAI index.

157

158 *Statistical Analyses*

159 We conducted non-parametric rank order analysis (ROA) to find group differences in the fiber  
160 measurements. To find the correlation of GOSE with fiber parameters, FLAIR DAI index, and  
161 factors such as age, initial GCS, and trauma coma databank (TCDB) CT classification, we  
162 performed Spearman correlation. The correlation analysis of GOSE and the categorical variable,  
163 gender, utilized Mann Whitney's test. A  $p < 0.05$  was considered a significant trend and  $p <$   
164  $0.005$  as statistically significant after correction for multiple comparisons.

165  
166 To predict GOSE from overall amount of injury in the three WM tracts, we first calculated fiber  
167 composite indices using STATIS,<sup>28</sup> a generalization of principal component analysis for data  
168 compression and integration, and then conducted partial least square (PLS) regression analysis  
169 for predicting GOSE in a mixed effects model.<sup>29,30</sup> We conducted two analyses in a mixed  
170 effects model: the fixed and random effects model analyses. The fixed effects model predicted  
171 individual GOSE scores based on information from the whole patient group. In the random  
172 effects model (or jackknife,  $n-1$  approach), each patient was taken out sequentially and the  
173 patient's GOSE score was predicted based on the remaining patients. Finally, the PLS GOSE  
174 factor that predicted GOSE best was correlated with the original DTI data to identify fiber  
175 parameters highly associated with the outcome.

176

177

**Results**

178 Twelve TBI patients were included in the study (8 males). Demographics, injury severity, MRI  
179 timing, and outcome assessments are summarized in Table 1. TCDB scores were 2 (diffuse  
180 injury) for 10 patients. One patient was rated 1 (normal) and one rated 3 (diffuse injury with

181 swell). Followup information was not obtained from one (8%) of the patients. Although all  
182 patients suffered severe TBI as rated by the initial GCS (range 1-8), the long-term functional  
183 outcome was more varied, ranging from good recovery (GOSE = 8) to death (GOSE = 1).

184  
185 The 3D reconstructions of CC, fornix, and PP (figure 2) were consistent with previous  
186 publications.<sup>25,31</sup> Only fiber parameters showing  $p < 0.005$  group differences are discussed. At  
187 least one fiber parameter of whole CC, all sub-areas of CC and PP, and fornix body were  
188 significantly different between the patients and controls with patients showing worse measures ( $p$   
189  $< 0.005$ , Tables 2).

190  
191 Spearman correlation revealed that at least one fiber parameter of whole CC, CC2 and CC4 had  
192 strong positive correlations with GOSE scores (Spearman's  $\rho > 0.76$ ,  $p < 0.005$ , Table 3). The  
193 Spearman's correlation between PLS regression predicted and actual GOSE was 0.91 ( $p < .001$ )  
194 in the fixed effects model, and 0.63 ( $p = 0.04$ ) in the random effects model. Table 3 also shows  
195 Spearman's  $\rho$  between fiber parameters of all WM tracts and the 1<sup>st</sup> factor of the PLS regression.  
196 In comparison, the two statistical methods found primarily similar results, although PLS  
197 regression detected more fiber parameters that were useful in predicting GOSE including the  
198 fiber count of CC2 and fiber volume of PVF. Figure 3 shows scatter plots of the mean FA of  
199 CC4 (left), and predicted GOSE in fixed (middle) and random (right) effects models against the  
200 GOSE.

201  
202 All patients had at least one WMH on their FLAIR images. The DAI index correlated  
203 marginally with the GOSE (Spearman's  $\rho = -0.53$ ,  $p = 0.10$ ). Age showed a significant

204 correlation with the GOSE (Spearman's  $\rho = -0.61, p < 0.05$ ). Gender, initial GCS, and TCBD  
205 scores did not correlate with the outcome in this small sample.

206

## 207 **Discussion**

208 In the present study, we explored techniques to obtain reliable and objective fiber measurements  
209 by refining fiber tracking methods. We performed 3D reconstruction of CC, fornix and PP using  
210 a multiple-ROI approach to increase inter-rater reliability.<sup>17,25</sup> To reduce subjectivity in slice  
211 selections, we utilized various anatomic landmarks for finding ROI slices. Our inter-rater  
212 reliability has reached 96% and above for all fiber measurements except for fornix crus (>89%).

213

214 Except for one quantitative study in chronic pediatric population,<sup>19</sup> previous DTI tractography  
215 studies have concentrated on visualizing fiber trajectory changes associated with TBI.<sup>18,32,33</sup>  
216 Additionally, among DTI studies using either ROI or DTI tractography approach, only one  
217 pediatric<sup>19</sup> and one adult TBI study<sup>20</sup> found an association between DTI measures obtained at the  
218 chronic stage of injury and outcome. In this pilot study, we tested whether tractography-based  
219 quantification of three WM structures vulnerable to DAI could detect lesions at an early stage  
220 after TBI and were associated with long-term outcome. Our results extended previous reports  
221 suggesting that DTI might detect loss of WM integrity due to DAI even at the beginning of the  
222 injury process and the acute DTI measurements were highly associated with long-term functional  
223 outcome. We found that at least one fiber parameter of the fornix body and all sub-regions of  
224 CC and PP were significantly worse in the patient than the control group. Despite a small  
225 number of patients with available GOSE scores ( $N = 11$ ), associations between the DTI  
226 measurements and GOSE were robust. Fiber measurements of the whole CC, CC2, and CC4 in

227 acute MRI scans were highly correlated with the GOSE scores. The correlation between the PLS  
228 predicted and actual GOSE scores was 0.91 ( $p < 0.001$ ) in fixed effects model and 0.63 ( $p =$   
229 0.04) in random effects model when incorporating all fiber measurements of the three tracts.  
230 Moreover, the fiber parameters that made significant contribution to the PLS regression  
231 corresponded to the fiber parameters with significantly high Spearman correlation coefficients  
232 with the GOSE. Figure 4 shows the WM regions found to be highly associated with the GOSE.  
233

234 In comparison, the correlation between the FLAIR DAI index and the GOSE only approached  
235 significance, and was similar to our previous findings in a larger data set.<sup>7</sup> Thus tractography-  
236 based quantification may be more useful than FLAIR lesion volume analysis and factors such as  
237 age, gender, initial GCS, TCDB CT classification in prognosis. The correlation between the  
238 GOSE and age was significant (Spearman's  $\rho = -0.61$ ,  $p = 0.046$ ) but not as strong as the  
239 correlation between the GOSE and DTI measurements.

240  
241 The detection of DAI in the CC, fornix body, and PP are consistent with previous DTI studies.  
242 Reduced FA values have been found in CC, internal and external capsules, and centrum  
243 semiovale at the acute stage of mild TBI<sup>15, 16</sup> and in fornix chronically.<sup>24</sup> The lack of DAI  
244 associated changes in fornix crura in the current study may be a technical limitation resulting  
245 from limited DTI image resolution.<sup>27</sup>  
246

247 One must exercise caution when interpreting fiber tracking results. The technique is relatively  
248 new and the FACT tracking algorithm employed in DTI Studio has limitations, particularly in  
249 the areas of crossing fibers. Failure or early termination in fiber propagation or fiber jumping

250 onto another tract may exist. The relatively small number of gradient encoding directions (19)  
251 that was state of the art at the time when scans were acquired might affect accuracy in tensor  
252 calculation. However, our findings suggest that the measurements from these DTI images had  
253 adequate signal-to-noise ratio for DAI diagnosis and prognosis. Other limitations are small  
254 sample size and the inclusion of only a subset of WM structures at risk. Investigations to address  
255 these limitations are underway.

256

257 The present study demonstrated that when implementing carefully designed fiber tracking  
258 methods, DTI tractography-based quantification may be useful for detecting DAI and predicting  
259 outcome. Our results also indicate that all six fiber parameters made unique contributions to the  
260 analyses.

261

262 Supported by: NIDRR H133 A020526, NIH R01 HD48179, NIH U01 HD42652 (to RD-A).

263

**References**

264

1. Langlois JA, Rutland-Brown W, Thomas K. Traumatic brain injury in the united states:

265

Emergency department visits, hospitalizations, and deaths. Atlanta Georgia: National center for

266

injury prevention and control, 2006.

267

2. Meythaler JM, Peduzzi JD, Eleftheriou E, Novack TA. Current concepts: Diffuse axonal

268

injury-associated traumatic brain injury. *Arch Phys Med Rehabil* 2001;82(10):1461-1471.

269

3. Gaetz M. The neurophysiology of brain injury. *Clin Neurophysiol* 2004;115(1):4-18.

270

4. Wilson S, Raghupathi R, Saatman KE et al. Continued in situ DNA fragmentation of

271

microglia/macrophages in white matter weeks and months after traumatic brain injury. *J*

272

*Neurotrauma* 2004;21(3):239-250.

273

5. Bigler ED. Distinguished neuropsychologist award lecture 1999. the lesion(s) in traumatic

274

brain injury: Implications for clinical neuropsychology. *Arch Clin Neuropsychol* 2001;16(2):95-

275

131.

276

6. Smith DH, Meaney DF, Shull WH. Diffuse axonal injury in head trauma. *J Head Trauma*

277

*Rehabil* 2003;18(4):307-316.

278

7. Marquez de la Plata,C., Ardelean A, Koovakkattu D et al. Magnetic resonance imaging of

279

diffuse axonal injury: Quantitative assessment of white matter lesion volume. *J Neurotrauma*

280

2007;24:591-598.

281

8. Scheid R, Walther K, Guthke T et al. Cognitive sequelae of diffuse axonal injury. *Arch Neurol*

282

2006;63(3):418-424.

- 283 9. Ashwal S, Babikian T, Gardner-Nichols J et al. Susceptibility-weighted imaging and proton  
284 magnetic resonance spectroscopy in assessment of outcome after pediatric traumatic brain injury.  
285 Arch Phys Med Rehabil 2006;87(12 Suppl 2):S50-8.
- 286 10. Metting Z, Rodiger LA, De Keyser J, van der Naalt J. Structural and functional neuroimaging  
287 in mild-to-moderate head injury. Lancet Neurol 2007;6(8):699-710.
- 288 11. Tong KA, Ashwal S, Holshouser BA et al. Diffuse axonal injury in children: Clinical  
289 correlation with hemorrhagic lesions. Ann Neurol 2004;56(1):36-50.
- 290 12. Basser PJ, Mattiello J, LeBihan D. Estimation of the effective self-diffusion tensor from the  
291 NMR spin echo. J Magn Reson B 1994;103(3):247-254.
- 292 13. Mac Donald CL, Dikranian K, Song SK et al. Detection of traumatic axonal injury with  
293 diffusion tensor imaging in a mouse model of traumatic brain injury. Exp Neurol  
294 2007;205(1):116-131.
- 295 14. Basser PJ, Pierpaoli C. Microstructural and physiological features of tissues elucidated by  
296 quantitative-diffusion-tensor MRI. J Magn Reson B 1996;111(3):209-219.
- 297 15. Arfanakis K, Haughton VM, Carew JD et al. Diffusion tensor MR imaging in diffuse axonal  
298 injury. AJNR Am J Neuroradiol 2002;23(5):794-802.
- 299 16. Inglese M, Makani S, Johnson G et al. Diffuse axonal injury in mild traumatic brain injury: A  
300 diffusion tensor imaging study. J Neurosurg 2005;103(2):298-303.
- 301 17. Mori S, van Zijl PC. Fiber tracking: Principles and strategies - a technical review. NMR  
302 Biomed 2002;15(7-8):468-480.

- 303 18. Xu J, Rasmussen IA, Lagopoulos J, Haberg A. Diffuse axonal injury in severe traumatic  
304 brain injury visualized using high-resolution diffusion tensor imaging. *J Neurotrauma*  
305 2007;24(5):753-765.
- 306 19. Wilde EA, Chu Z, Bigler ED et al. Diffusion tensor imaging in the corpus callosum in  
307 children after moderate to severe traumatic brain injury. *J Neurotrauma* 2006;23(10):1412-1426.
- 308 20. Kraus MF, Susmaras T, Caughlin BP et al. White matter integrity and cognition in chronic  
309 traumatic brain injury: A diffusion tensor imaging study. *Brain* 2007.
- 310 21. Wilson JT, Pettigrew LE, Teasdale GM. Structured interviews for the glasgow outcome scale  
311 and the extended glasgow outcome scale: Guidelines for their use. *J Neurotrauma*  
312 1998;15(8):573-585.
- 313 22. Hudak AM, Caesar RR, Frol AB et al. Functional outcome scales in traumatic brain injury: A  
314 comparison of the glasgow outcome scale (extended) and the functional status examination. *J*  
315 *Neurotrauma* 2005;22(11):1319-1326.
- 316 23. Huisman TA, Schwamm LH, Schaefer PW et al. Diffusion tensor imaging as potential  
317 biomarker of white matter injury in diffuse axonal injury. *AJNR Am J Neuroradiol*  
318 2004;25(3):370-376.
- 319 24. Nakayama N, Okumura A, Shinoda J et al. Evidence for white matter disruption in traumatic  
320 brain injury without macroscopic lesions. *J Neurol Neurosurg Psychiatry* 2006;77(7):850-855.
- 321 25. Catani M, Howard RJ, Pajevic S, Jones DK. Virtual in vivo interactive dissection of white  
322 matter fasciculi in the human brain. *Neuroimage* 2002;17(1):77-94.

- 323 26. Huang H, Zhang J, Jiang H et al. DTI tractography based parcellation of white matter:  
324 Application to the mid-sagittal morphology of corpus callosum. *Neuroimage* 2005;26(1):195-  
325 205.
- 326 27. Concha L, Gross DW, Beaulieu C. Diffusion tensor tractography of the limbic system. *AJNR*  
327 *Am J Neuroradiol* 2005;26(9):2267-2274.
- 328 28. Abdi H, Valentin D. *STATIS*. Thousand Oaks, CA: SAGE Publications, Inc., 2007.
- 329 29. McIntosh AR, Lobaugh NJ. Partial least squares analysis of neuroimaging data: Applications  
330 and advances. *Neuroimage* 2004;23 Suppl 1:S250-63.
- 331 30. Abdi H. *Partial least square regression (PLS regression)*. Thousand Oaks, CA: SAGE  
332 Publications, Inc., 2007.
- 333 31. Wakana S, Jiang H, Nage-Poetscher LM et al. Fiber tract-based atlas of human white matter  
334 anatomy. *Radiology* 2004;230(1):77-87.
- 335 32. Naganawa S, Sato C, Ishihara S et al. Serial evaluation of diffusion tensor brain fiber tracking  
336 in a patient with severe diffuse axonal injury. *AJNR Am J Neuroradiol* 2004;25(9):1553-1556.
- 337 33. Le TH, Mukherjee P, Henry RG et al. Diffusion tensor imaging with three-dimensional fiber  
338 tractography of traumatic axonal shearing injury: An imaging correlate for the posterior callosal  
339 "disconnection" syndrome: Case report. *Neurosurgery* 2005;56(1):189.

340

341

342

343 Figure 1. Fornix body reconstruction of a representative control (**A, B**) and patient (**C, D**). The  
344 first ROI was placed on an axial slice 6mm superior to the anterior commissure (**A, C**). The  
345 second ROI was place on the most posterior coronal slice in which the fornix remained as one  
346 bundle (**B, D**). The ROI operation used was CUT.

347

348 Figure 2. Representative fiber tractography results from a control (left) and patient (right). CC  
349 (top) is parcellated into areas 1-4 as shown by the corresponding colors yellow, orange, green, or  
350 blue. Fornix body and inferior crura are colored in yellow (middle). PP (bottom) is parcellated  
351 into PVF (yellow), PDF (orange), PPar (green), and POcc (blue). The patient did not have  
352 cortical contusions on CT scanning, but some shear hemorrhages were noted.

353

354 Figure 3. Plots of the mean FA of CC4 (left), and the predicted GOSE in fixed (middle) and  
355 random (right) effects models against the GOSE.

356

357 Figure 4. Overlay of fiber tracts highly associated with the GOSE on a representative FA map of  
358 a normal control. CC2 and CC4 are in orange. PVF is in blue.

359

360

361

362

363

364

365

366

367

368

369

370

371 Table 1. Patient demographic information.

	<b>Mean</b>	<b>SD</b>	<b>Median</b>	<b>Range</b>
<b>Age (years)</b>	26	8.1	25	16-37
<b>GCS</b>	4.4	2.1	3	3-8
<b>GOSE</b>	4.4	2.2	4	1-8
<b>Time to scan (days)</b>	6.7	4.2	6.5	0-15
<b>Time to followup (months)</b>	8.2	1.6	9	6-11

372 GCS = Glasgow Coma Scale; GOSE = Glasgow Outcome Scale-Extended; SD = Standard  
 373 Deviation.

374

375

376

377

378

379

380

381

382

383

384

385

386

387

388

389

390

391

392

393

394

395

396

397

398

399

400

401

402 Table 2. Group comparisons (patients vs. controls) of fiber measurements.

Fiber Parameters	Controls Mean ± SD	Patients Mean ± SD	p Value of ROA	Controls Mean ± SD	Patients Mean ± SD	p Value of ROA
	<b>CC</b>			<b>PVF</b>		
Mean FA	0.59 ± 0.02	0.56 ± 0.02	<b>&lt; 0.001</b>	0.52 ± 0.02	0.51 ± 0.02	-
Tensor Trace (µm <sup>2</sup> /ms)	2.18 ± 0.07	2.22 ± 0.12	-	2.07 ± 0.07	2.20 ± 0.09	<b>&lt; 0.001</b>
Fiber Count (1,000)	12 ± 1.8	8.8 ± 1.6	<b>&lt; 0.001</b>	232 ± 190	182 ± 172	-
Mean Length (mm)	94 ± 5	89 ± 6	0.01	114 ± 14	107 ± 12	-
Fiber Volume (1,000 voxels)	26 ± 3.8	21 ± 3.4	<b>&lt; 0.001</b>	2.3 ± 1.1	1.8 ± 1.2	-
FDI (fiber count/voxel)	43 ± 3.7	40 ± 3.4	0.01	10 ± 5.4	8.7 ± 4.3	-
	<b>CC: Genu</b>			<b>PDF</b>		
Mean FA	0.58 ± 0.02	0.54 ± 0.03	<b>0.003</b>	0.55 ± 0.02	0.52 ± 0.04	<b>0.002</b>
Tensor Trace (µm <sup>2</sup> /ms)	2.20 ± 0.07	2.29 ± 0.19	<b>0.004</b>	2.03 ± 0.07	2.12 ± 0.07	<b>0.002</b>
Fiber Count (1,000)	3.9 ± 0.6	3.2 ± 0.7	0.02	1084 ± 392	575 ± 355	<b>0.002</b>
Mean Length (mm)	90 ± 8	87 ± 6	-	118 ± 8	112 ± 11	-
Fiber Volume (1,000 voxels)	7.6 ± 1.2	6.7 ± 1.3	-	5.2 ± 1.5	3.1 ± 1.4	<b>0.001</b>
FDI (fiber count/voxel)	51 ± 4.8	46 ± 5.1	0.01	17 ± 3.8	12 ± 5.0	0.01
	<b>CC: Anterior Body</b>			<b>PPar</b>		
Mean FA	0.54 ± 0.02	0.52 ± 0.04	-	0.55 ± 0.02	0.52 ± 0.03	<b>0.002</b>
Tensor Trace (µm <sup>2</sup> /ms)	2.21 ± 0.11	2.22 ± 0.17	-	2.05 ± 0.07	2.15 ± 0.08	<b>0.002</b>
Fiber Count (1,000)	1.3 ± 0.4	1.0 ± 0.4	0.01	713 ± 440	500 ± 426	-
Mean Length (mm)	65 ± 11	59 ± 13	-	115 ± 9	112 ± 9	-
Fiber Volume (1,000 voxels)	3.7 ± 1.0	2.7 ± 1.0	<b>0.0048</b>	4.5 ± 1.8	2.9 ± 1.8	0.02
FDI (fiber count/voxel)	21 ± 4.5	19 ± 4.0	-	14 ± 3.3	13 ± 5.3	-
	<b>CC: Posterior Body</b>			<b>POcc</b>		
Mean FA	0.53 ± 0.04	0.49 ± 0.06	0.02	0.56 ± 0.02	0.52 ± 0.03	<b>0.001</b>
Tensor Trace (µm <sup>2</sup> /ms)	2.29 ± 0.17	2.28 ± 0.24	-	2.12 ± 0.08	2.17 ± 0.08	0.048
Fiber Count (1,000)	1.4 ± 0.6	0.9 ± 0.4	0.01	134 ± 131	164 ± 131	-
Mean Length (mm)	75 ± 15	73 ± 19	-	116 ± 15	107 ± 11	-
Fiber Volume (1,000 voxels)	4.0 ± 1.4	2.9 ± 1.2	<b>0.003</b>	1.7 ± 1.0	1.8 ± 0.8	-
FDI (fiber count/voxel)	24 ± 6.2	21 ± 6.7	-	7.3 ± 3.5	8.6 ± 3.4	-
	<b>CC: Splenium</b>			<b>Fornix Body</b>		
Mean FA	0.62 ± 0.02	0.57 ± 0.03	<b>&lt; 0.001</b>	0.58 ± 0.03	0.52 ± 0.09	0.01
Tensor Trace (µm <sup>2</sup> /ms)	2.17 ± 0.09	2.17 ± 0.15	-	3.38 ± 0.31	3.27 ± 0.35	-
Fiber Count (1,000)	4.8 ± 0.9	3.6 ± 0.6	<b>&lt; 0.001</b>	107 ± 43	55 ± 32	<b>&lt; 0.001</b>
Mean Length (mm)	110 ± 7	101 ± 9	0.01	25 ± 5	22 ± 4	0.03
Fiber Volume (1,000 voxels)	12.1 ± 23	9.1 ± 1.5	<b>&lt; 0.001</b>	172 ± 44	120 ± 39	<b>&lt; 0.001</b>
FDI (fiber count/voxel)	46 ± 4.6	43 ± 4.4	0.02	16 ± 4.9	9.4 ± 3.8	<b>0.001</b>

403 Bold fonts,  $p < .005$ ; -,  $p \geq .05$ .

404 CC = Corpus callosum; PVF = Peduncular projections to ventral frontal cortex; PDF =  
 405 Peduncular projections to dorsal frontal cortex; PPar = Peduncular projections to parietal cortex;  
 406 POcc = Peduncular projections to occipital cortex; FA = Fractional anisotropy; FDI = Fiber  
 407 density index; ROA = Rank order analysis; GOSE = Glasgow outcome scale-extended; PLS =  
 408 Partial least square; SD = Standard deviation.

409

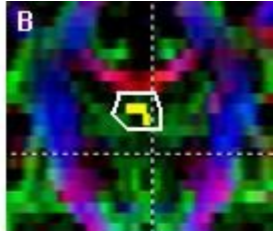
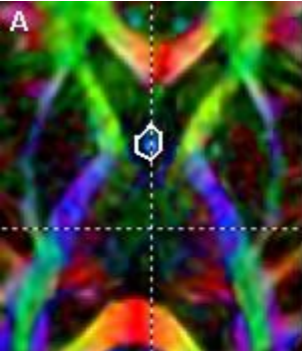
410

411 Table 3. Correlation of fiber measurements with GOSE and PLS factor 1.

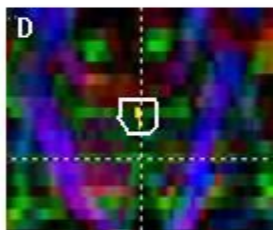
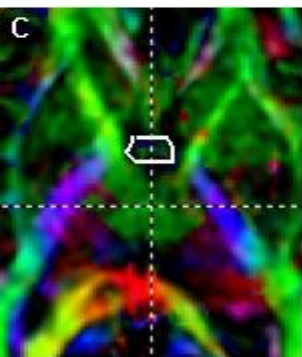
Fiber Parameters	Spearman's $\rho$ with GOSE	Spearman's $\rho$ with PLS Factor 1	Spearman's $\rho$ with GOSE	Spearman's $\rho$ with PLS Factor 1
	<b>CC</b>		<b>PVF</b>	
Mean FA	<b>0.86</b>	<b>0.92</b>	-	-
Tensor Trace	-	-	-	-
Fiber Count	<b>0.80</b>	0.73	-	0.77
Mean Length	-	-	-	-
Fiber Volume	0.72	-	-	<b>0.79</b>
FDI	0.63	0.67	-	0.66
	<b>CC: Genu</b>		<b>PDF</b>	
Mean FA	-	-	-	-
Tensor Trace	-	-	-	-
Fiber Count	-	-	-	-
Mean Length	-	-	-	-
Fiber Volume	-	-	-	-
FDI	-	0.76	-	-
	<b>CC: Anterior Body</b>		<b>PPar</b>	
Mean FA	-	-	-	-
Tensor Trace	-	-	-	-
Fiber Count	0.74	<b>0.81</b>	-	-
Mean Length	<b>0.91</b>	<b>0.93</b>	-	0.62
Fiber Volume	0.73	0.76	-	-
FDI	<b>0.84</b>	<b>0.86</b>	-	-
	<b>CC: Posterior Body</b>		<b>POcc</b>	
Mean FA	0.64	0.66	0.69	0.67
Tensor Trace	-	-	-	-
Fiber Count	-	-	-	-
Mean Length	0.61	-	0.73	-
Fiber Volume	-	-	-	-
FDI	-	-	0.66	-
	<b>CC: Splenium</b>		<b>Fornix Body</b>	
Mean FA	<b>0.92</b>	<b>0.86</b>	-	-
Tensor Trace	-	-	-	-
Fiber Count	-	-	-	0.62
Mean Length	-	-	-	-
Fiber Volume	-	-	-	-
FDI	0.71	-	-	0.66

412 Bold fonts,  $p < .005$ ; -,  $p \geq .05$ .

413 CC = Corpus callosum; PVF = Peduncular projections to ventral frontal cortex; PDF =  
 414 Peduncular projections to dorsal frontal cortex; PPar = Peduncular projections to parietal cortex;  
 415 POcc = Peduncular projections to occipital cortex; FA = Fractional anisotropy; FDI = Fiber  
 416 density index; ROA = Rank order analysis; GOSE = Glasgow outcome scale-extended; PLS =  
 417 Partial least square; SD = Standard deviation.



Fornix body ROI 1 (A) and ROI 2 (B) of a control.



Fornix body ROI 1 (C) and ROI 2 (D) of a patient.

Figure 1

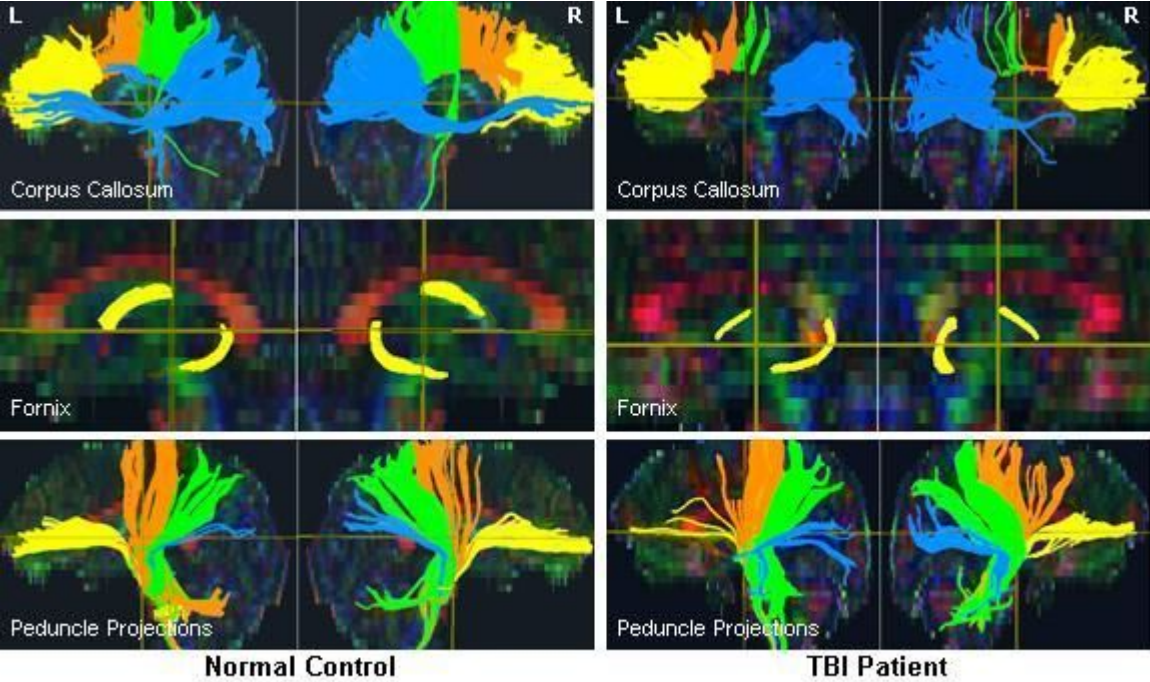


Figure 2

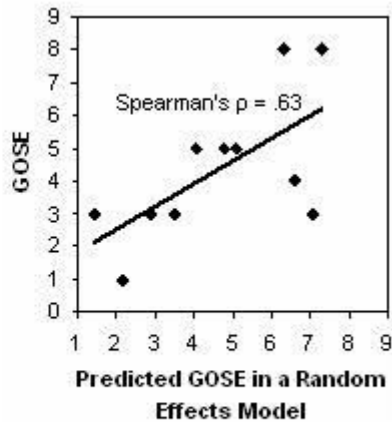
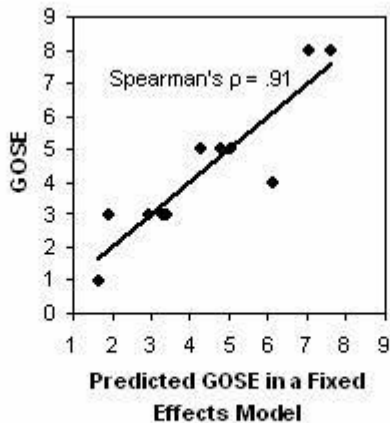
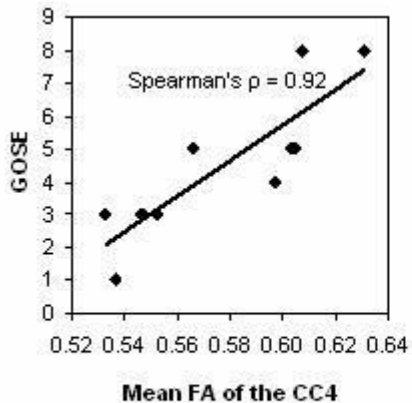


Figure 3

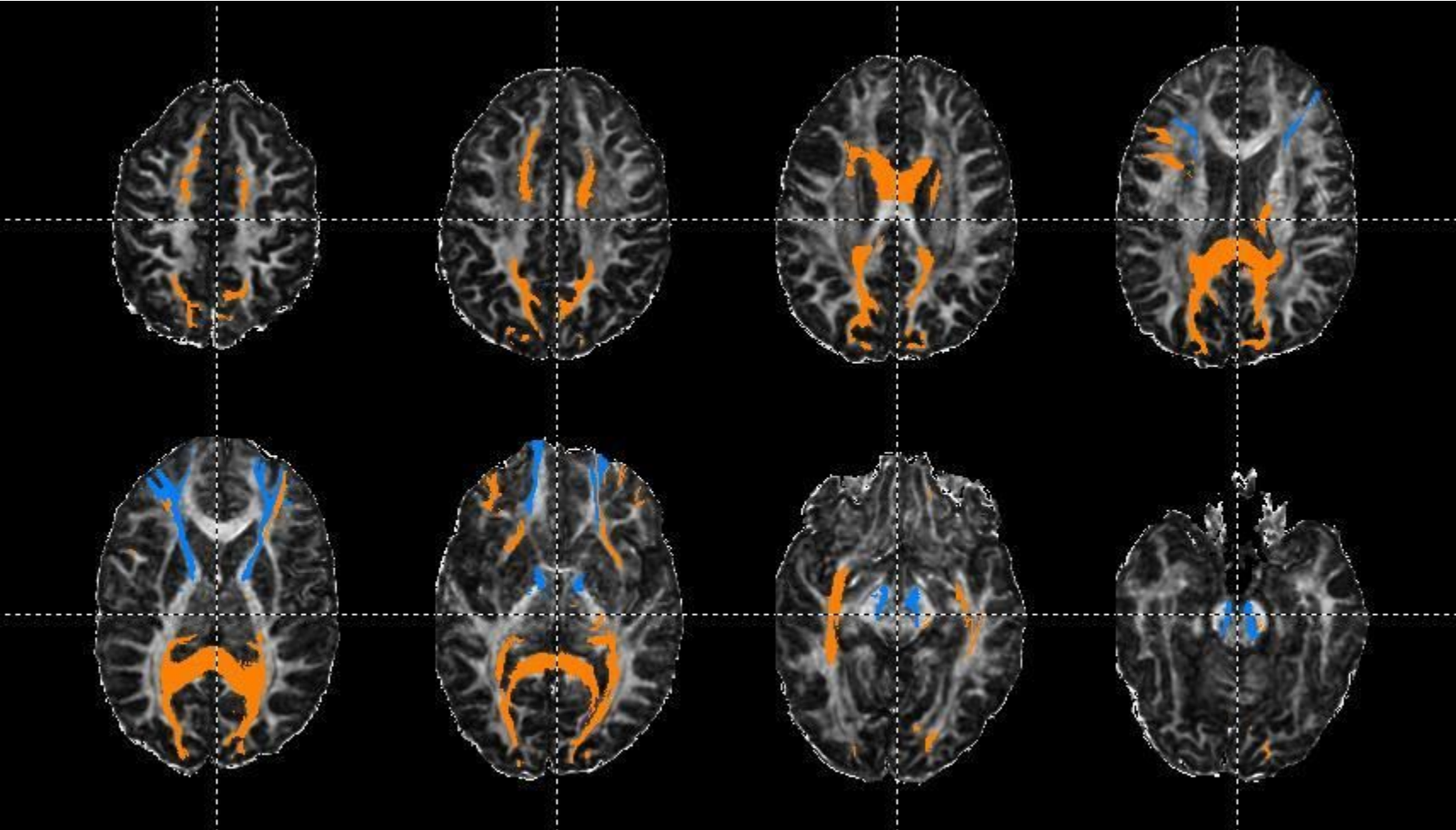


Figure 4